

Development of the Resolved Fluid-Solid SPH Coupling using Rigid Body Dynamics

Hae Yoon Choi^a, Eung Soo Kim^{a*}

^a Department of Nuclear Engineering, Seoul National University, 1 Gwanak-ro, Gwanak-gu, Seoul, South Korea

*Corresponding author: kes7741@snu.ac.kr

1. Introduction

The interests in the nuclear safety analysis related to the flooding accidents is increasing after the Fukushima accident. Solid debris generated by flooding or nuclear plant equipment like emergency diesel generator may move due to fluid behavior and cause damage. In addition, fluid-solid interaction may occur in the debris behavior caused by the FCI phenomenon in the ex-vessel pre-flooded cavity during a severe accident. [1-3] So, the analysis of the interaction between solid debris and fluid is important in nuclear safety respect. These debris transport phenomena include the solid bodies of arbitrary shape, and interaction between fluid-solid as well as solid-solid. Therefore, the SPH method coupled with solid analysis which has advantages of easy tracking of the phase boundary can be an effective approach for debris transport simulations

For various nuclear applications, a fully resolved Rigid Body Dynamics (RBD) model was developed based on Discrete Element Method (DEM) method. By coupling SPH-RBD using GPU parallelization, the high resolution 3D simulation between the liquid phase and solid phase could be possible.

2. Smoothed Particle Hydrodynamics (SPH)

The SPH method is one of the Lagrangian analysis methods, which analyzes the fluid flows by calculating the motion of individual particles. The particles have each property and are calculated through the weight function over the neighboring particles within the support area (or smoothing length). (Fig. 1) This SPH method has advantages in handling free surface flow, multi-fluid (phase) flow, and high deformable geometry due to its Lagrangian nature.

2.1. SPH Basics

The SPH particle approximation is performed by discretizing the kernel function which has the characteristics of the delta function.

$$f(r_i) = \sum_j \frac{m_j}{\rho_j} f_j W_{ij} \quad (1)$$

f_i is a function at the position i , W_{ij} is a kernel function, j is a neighboring particle within the smoothing length, and m, ρ means mass and density respectively.

The first derivative of the field function $f(r)$ is expressed as a function of kernel derivatives for all the particles in the support domain of particle i . [4]

$$\nabla f(r_i) = \sum_j \frac{m_j}{\rho_j} f_j \nabla W_{ij} \quad (2)$$

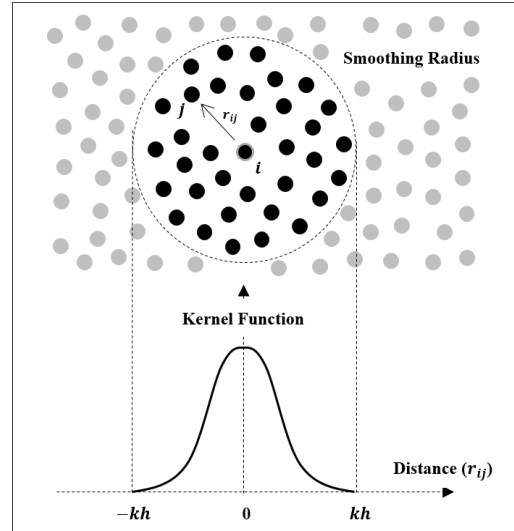


Fig 1. SPH Kernel Approximation

2.2. Governing Equations

The SPH method satisfies the mass and momentum conservation and can be expressed in the form of equations (3) and (4).

$$\frac{d\rho}{dt} = -\rho \nabla \cdot \vec{u} \quad (3)$$

$$\frac{d\vec{u}}{dt} = -\frac{1}{\rho} \nabla P + \frac{\mu}{\rho} \nabla^2 \vec{u} + \vec{g} \quad (4)$$

\vec{u}, P, μ, \vec{g} denote velocity field, pressure, dynamic viscosity, and gravitational constant, respectively.

Table 1. shows the SPH expression of the governing equations and physical models used in this study. In the general SPH method, the calculation is carried out assuming weak compressibility of the fluid, so the Tait equation is used for the equation of state (EOS).

2.3. Multi-fluid Models

In multi-fluid calculation, a discontinuity of physical properties occurs at the fluid interface. Since the SPH pressure force calculation is based on a function of density, a large density difference near the boundary causes non-physical pressure force. Therefore, a normalized density formulation is introduced to ensure stability by replacing the density (ρ) with the normalized density (ρ/ρ_0). [5]

$$\left(\frac{\rho}{\rho_0}\right)_i = \sum_j \frac{m_j}{\rho_{0,j}} W_{ij} \quad (5)$$

Table 1. SPH Formulations

Mass Conservation (normalized density)	
	$\rho_i = \rho_{ref,i} \sum_j \frac{m_j}{\rho_{ref,j}} W_{ij}$
Momentum Conservation	
Pressure force	$\left(\frac{d\vec{u}}{dt}\right)_i = \sum_j -\frac{m_j}{\rho_i \rho_j} (P_j + P_i) \nabla W_{ij}$
Viscous force	$\left(\frac{d\vec{u}}{dt}\right)_i = \sum_j -\frac{4m_j}{\rho_i \rho_j} \frac{\mu_i \mu_j}{\mu_i + \mu_j} \frac{\vec{r}_{ij} \cdot \nabla W_{ij}}{r_{ij}^2 + \varepsilon^2} (\vec{u}_i - \vec{u}_j)$
Surface tension force	$\left(\frac{d\vec{u}}{dt}\right)_i = \sum_j \frac{\sigma_a}{\rho_i} \kappa_{ij} (\nabla c)_{ij}$
Equation of State	
	$P = \frac{c_0^2 \rho_0}{\gamma} \left[\left(\frac{\rho}{\rho_0}\right)^\gamma - 1 \right]$

3. Rigid Body Dynamics (RBD)

In this study, solid modeling with irregular shape was performed by applying the concept that a rigid body doesn't change its shape by applied external forces. The penalty-based spring dashpot model which has been widely used in the DEM analysis is applied to implement the rigid body motion in this study. [6-11]

3.1. Rigid Body in SPH

In the SPH method, rigid bodies are composed of many particles and analyzed by collisions between rigid bodies. (Fig. 2) The translational and rotational motion of the rigid body can be presented by adding up individual forces (\vec{F}_c) that all the particles constituting the rigid body receive during the collisions. The interactive forces between colliding particles are covered in the next section.

$$M_I \frac{d\vec{v}_I}{dt} = \sum_l \sum_i (\vec{F}_{c_i} + m_i \vec{g}) \quad (8)$$

$$I \frac{d\vec{\omega}_I}{dt} = \sum_l \vec{\tau}_I = \sum_l \sum_i (\vec{r}_i - \vec{r}_{cm}) \times \vec{F}_{c_i} \quad (9)$$

The subscript I, i refers to the rigid body I and the individual particles i constituting rigid body I.

3.2. Spring-dashpot Model

The collision between rigid bodies is solved by spring-dashpot model allowing a slight overlap in the particles. A spring force, a damping force, and a frictional force are calculated in the normal and tangential direction of the collision. Contact forces are as follows. [6]

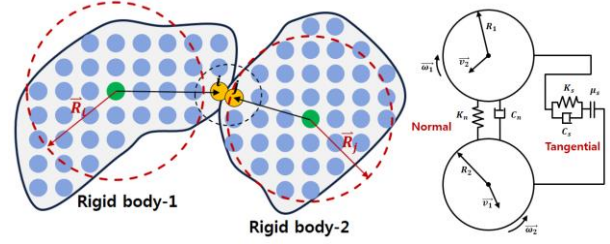


Fig 2. Rigid Body Collision in SPH Method

$$\vec{f}_n = \vec{f}_n^r + \vec{f}_n^d = k_n \delta_n \hat{n} + c_n \vec{v}_n \quad (10)$$

$$\vec{f}_t = \min \begin{cases} \vec{f}_t^r + \vec{f}_t^d = k_t \delta_t \hat{t} + c_t \vec{v}_t \\ \vec{f}_t^{friction} = -\mu |\vec{f}_n| \hat{t} \end{cases} \quad (11)$$

The superscript r, d means repulsive, damping force and the subscript n, t means normal, tangential direction. k, c is the coefficient for spring and damping. δ means the overlap and \vec{v}_n, \vec{v}_t denotes relative normal, tangential velocity vector of the colliding particles.

4. SPH-RBD Coupling

Multi-phase flow analysis can be possible through SPH-Rigid Body coupling. In this study, the resolved method was adopted and details are as follows.

4.1. Fully Resolved SPH-Rigid Body Coupling

The implemented resolved method satisfies the 1st principle, so the analysis is possible even when the solid phase much larger than the fluid particle size. And the interfaces of fluid phase and solid phase are completely separated. Fluid-solid interaction can be easily performed by calculating the pressure force (f_p), viscous force (f_v), and surface tension force (f_s) of the fluid particles applied to the surface particle of the rigid bodies without surface integral. Fig. 3 shows all kind of particle interactions in the SPH-RBD interaction model.

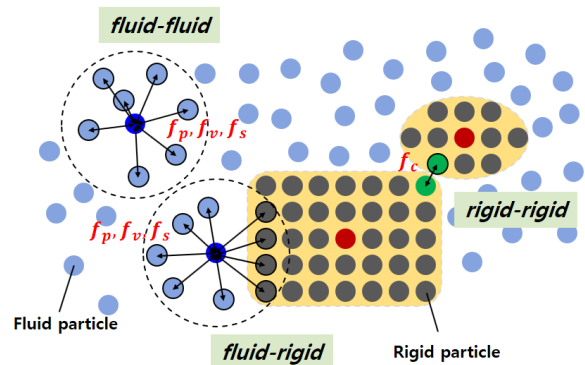


Fig 3. Schematic of fluid-rigid particle interactions

4.2. Algorithm of SPH-RBD Model

In addition to the existing fluid-fluid interactions, rigid-rigid interactions and fluid-rigid interactions have been added. A summation operation of all the particles constituting the rigid body is required for interactions of rigid bodies. In order to efficiently calculate the many particles constituting the rigid bodies, the GPU-based parallelization was carried out and shows good high speed performance. The overall algorithm of SPH-RBD coupling analysis is shown in Fig. 4.

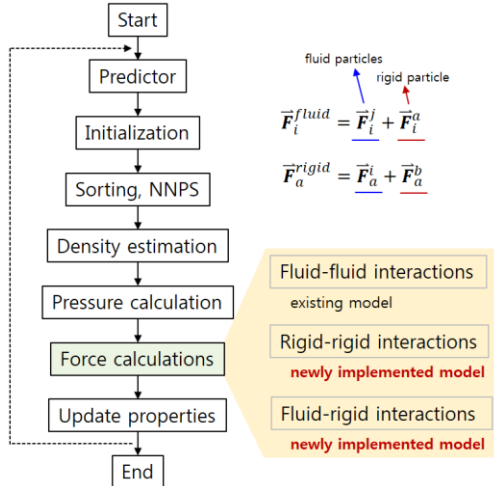


Fig 4. Algorithm for SPH-RBD Coupling Analysis

5. V&V Simulations

The validation of the RBD modeling and SPH-RBD coupling has been performed. Details are as follows.

5.1. Validation for Rigid-Rigid Interactions

Fig. 5 shows the elastic collision analysis of a solid box. The solid box consists of 100 SPH particles, and the fixed boundary is considered as a rigid body with infinite mass. Also, the rigid body slip on the slope simulation was carried out for tangential collision. (Fig. 6)

In both simulations, results were in good agreement with the analytic solution.

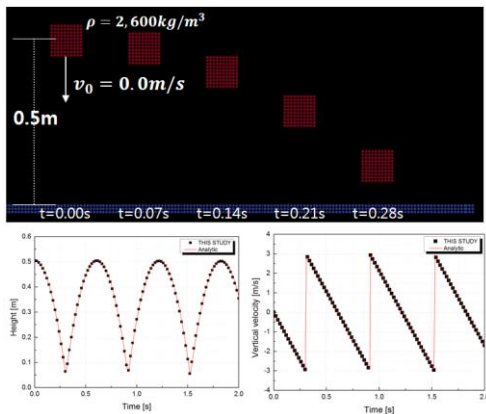


Fig 5. Results of elastic rigid body collision [12]

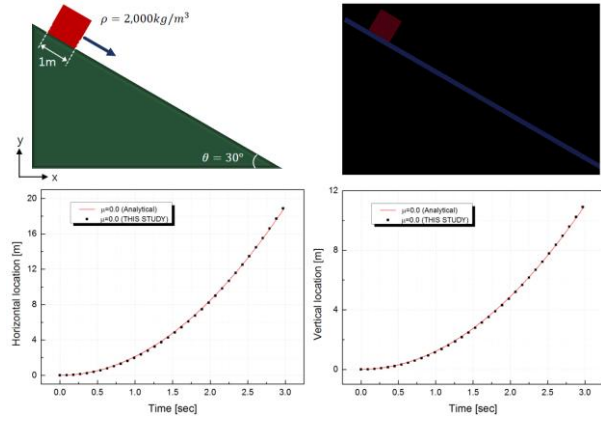


Fig 6. Results of rigid body sliding on a slope [13]

5.2. Validation for Fluid-Rigid Interactions

In order to simulate the interaction between the fluid and the rigid body, the verification tests were performed for the case where rigid body fall into the water and rise in the water.

Since the buoyancy force of the rigid body is proportional to the surface area in contact with the fluid, the 3D analysis shows much better results than 2D simulation. Fig. 7-8 show the result of the vertical location of the rigid body.

Based on the contact force in rigid collision and coupling on SPH-RBD, 3-dimensional multi-rigid body dambreak was simulated. (Fig. 9)

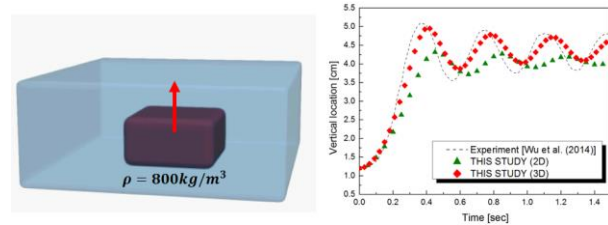


Fig 7. Results of the floating rigid body [12]

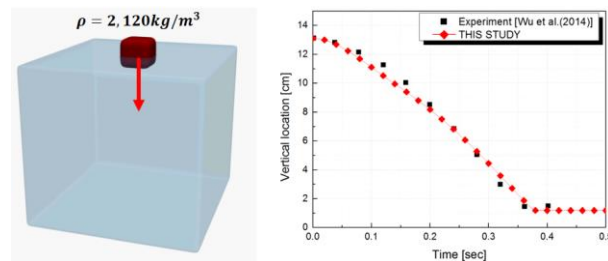


Fig 8. Results of the falling rigid body [12]

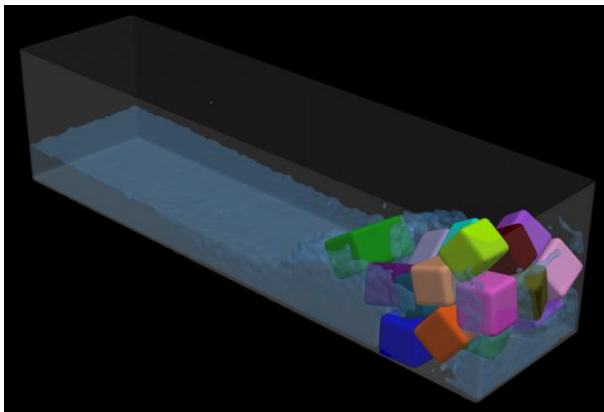


Fig 9. 3D multi-rigid body dambreak simulation

6. Summary

In this study, rigid body dynamics which analyzes the motion of irregular solid phase was implemented in the SOPHIA code. Also, an analysis system for multi-phase (fluid-solid) flow was developed through the resolved coupling between SPH and RBD, and GPU-based parallelization was carried out for the high performance of simulations. V&V simulations were carried out and results were in good agreement with the analytic solution. Additional verification and validation on multi-phase, multi-rigid body integrated simulation will be conducted using a two-way coupled SPH-RBD SOPHIA code.

ACKNOWLEDGEMENT

This work was supported by the Nuclear Safety Research Program through the Korea Foundation Of Nuclear Safety (KoFONS) using the financial resource granted by the Nuclear Safety and Security Commission (NSSC) of the Republic of Korea. (No. 1903003)

REFERENCES

- [1] Ikeda, Hirokazu, et al. "Numerical analysis of jet injection behavior for fuel-coolant interaction using particle method." *Journal of nuclear science and technology* 38.3 (2001): 174-182.
- [2] Jin, Youngho, and Kwangil Ahn. "Improvement of Diagnostic Flow Chart in Severe Accident Management Guidance of OPR1000 Reflecting Fukushima Accident Experience." *Transactions of the Korean Nuclear Society Spring Meeting*. 2014.
- [3] OECD/NEA SERENA Final Report, 2007. SERENA- Steam Explosion Resolution for Nuclear Applications. NEA/CSNI/R (2007)11.
- [4] G. R. Liu, M. B. Liu, "Smoothed Particle Hydrodynamics: a meshfree particle methods", 2003.
- [5] Jo, Young Beom, et al. "SOPHIA: Development of Lagrangian-based CFD code for nuclear thermal-hydraulics and safety applications." *Annals of Nuclear Energy* 124 (2019): 132-149.

[6] Johnson, K. L. "Contact Mechanics", Cambridge University Press, Cambridge, 1985."

[7] Cundall, Peter A., and Otto DL Strack. "A discrete numerical model for granular assemblies." *geotechnique* 29.1 (1979): 47-65.

[8] Zhu, H. P., et al. "Discrete particle simulation of particulate systems: theoretical developments." *Chemical Engineering Science* 62.13 (2007): 3378-3396.

[9] Peng, Bo. "Discrete element method (DEM) contact models applied to pavement simulation." *Diss. Virginia Tech*, 2014.

[10] Raji, Abdulganij Olayinka. "Discrete element modelling of the deformation of bulk agricultural particulates." (1999).

[11] DEM Solutions Ltd. 2016. EDEM 2.6 Theory Reference Guide. Edinburgh: DEM Solutions Ltd.

[12] Qiu, Liu-Chao, Yi Liu, and Yu Han. "A 3D simulation of a moving solid in viscous free-surface flows by coupling SPH and DEM." *Mathematical Problems in Engineering* 2017 (2017).

[13] Zhan, Ling, et al. "A SPH framework for dynamic interaction between soil and rigid body system with hybrid contact method." *International Journal for Numerical and Analytical Methods in Geomechanics* (2020).